

## Control system for 5 MW neutral beam ion source for SST1

G. B. Patel,<sup>a)</sup> Raja Onali, Vivek Sharma,<sup>b)</sup> S. Suresh, V. Tripathi, M. Bandyopadhyay, N. P. Singh, Dipal Thakkar, L. N. Gupta, M. J. Singh, P. J. Patel, A. K. Chakraborty, U. K. Baruah, and S. K. Mattoo

*Institute for Plasma Research, Bhat, Gandhinagar, Gujarat, India-382428*

(Received 20 July 2005; accepted 11 November 2005; published online 12 January 2006)

This article describes the control system for a 5 MW ion source of the NBI (neutral beam injector) for steady-state superconducting tokamak-1 (SST-1). The system uses both hardware and software solutions. It comprises a DAS (data acquisition system) and a control system. The DAS is used to read the voltage and current signals from eight filament heater power supplies and 24 discharge power supplies. The control system is used to adjust the filament heater current in order to achieve an effective control on the discharge current in the plasma box. The system consists of a VME (Verse Module Eurocard) system and C application program running on a VxWorks™ real-time operating system. A *PID* (proportional, integral, and differential) algorithm is used to control the filament heater current. Experiments using this system have shown that the discharge current can be controlled within 1% accuracy for a *PID* loop time of 20 ms. Response of the control system to the pressure variation of the gas in the chamber has also been studied and compared with the results obtained from those of an uncontrolled system. The present approach increases the flexibility of the control system. It not only eases the control of the plasma but also allows an easy changeover to various operation scenarios. © 2006 American Institute of Physics. [DOI: 10.1063/1.2149607]

### I. INTRODUCTION

New generation steady-state fusion machines are under construction.<sup>1-4</sup> These machines will have operation time scales as long as 1000 s. Auxiliary heating of plasmas in these machines is based upon the use of rf power and neutral beams. Behavior of these machines over such long time scales is not known at present, particularly when plasmas produced in the divertors are intensely heated to an ion temperature  $\sim 1$  keV.<sup>5,6</sup> This is because the long-term behavior of plasma-wall interaction is not known. Under such circumstances, it becomes essential to deliver controlled heating power in response to the change in the plasma behavior due to plasma-wall interactions.

In earlier machines, the emphasis was to provide steady power at a given beam energy over a period of not more than a few tens of seconds. There was no necessity of delivering it in response to any activity related to the long-term change in the plasma behavior. Consequently, the control system was simple and it mostly grew around the use of hardwired electronics. Later, when programmable systems became available, PLC (programmable logic control) was used for such applications.<sup>7</sup> The major drawback with such systems is their long loop time  $>50$  ms. Reduction of loop time to  $\sim 1$  ms is possible with hardware control logic, implemented with a large number of operational amplifiers. But, such systems are less flexible and it is difficult to change the operation parameters. Further, other systems like CAMAC, VME, VXI, or other PCI-based systems have to be deployed for data acquisition.<sup>8</sup>

For our system we propose the use of a VME system for control, data acquisition, and for generating a timing sequence, which is also used in other subsystems of the NBI (Neutral Beam Injector). The efficacy of such a system has been tested on a real prototype plasma box. Section II of this article describes the requirements for the data acquisition and control system for the ion source. Section III gives a detailed overview of the hardware and software configuration, the control algorithm, and the control software. Results highlighting the system performance are described in Sec. IV.

### II. EXPERIMENT AND DATA ACQUISITION AND CONTROL SYSTEM

#### A. Experimental setup

A schematic of the plasma box is shown in Fig. 1(a). It is a cylindrical stainless-steel chamber of 45 cm diameter and 43 cm length, and is provided with 24 columns of samarium cobalt magnets with magnetic field  $B_{\max}$  of  $\sim 3.6$  kG on the pole surface. The back plate, 5.4 cm away from the cylindrical array of 24 filaments, is also provided with 11 columns of magnets. The magnets provide the multipole confinement. The field on the back plate joins the field on the curved surface without causing extra loss cusps at the corners. Hairpin-type tungsten filaments, 0.1 cm diameter and 16 cm length, are used as the primary electron source.

The chamber wall acts as the anode for the discharge. The background magnetic field due to the multipole is below 3 G at the filament tip. Figure 1(b) shows the arrangement of the filaments and the locations of the cusps in the plasma box.

Figure 2 shows a schematic arrangement of the power supplies used for the discharge and heating of a group of

<sup>a)</sup>Electronic mail: gaurav@ipr.res.in

<sup>b)</sup>Presently working at DRDO, Bangalore, India.

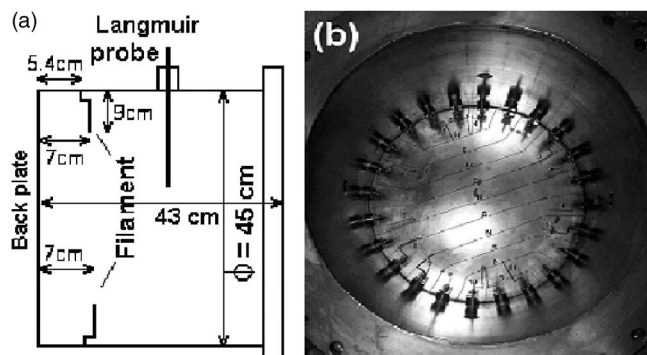


FIG. 1. (a) Schematic of plasma box. (b) Photograph of plasma box showing filament positions and magnet cusp lines on the back plate.

three filaments. A similar arrangement exists for the 24 filaments in the plasma box. The ac (400 Hz) filament heater power supply is rated for 15 V, 160 A. Each filament in the group of three is connected to the secondary of a three-phase transformer. The primary of the transformer is connected to the filament power supply. For discharge purposes, each filament has a separate discharge power supply. This supply is rated for 160 V, 100 A dc and can be operated in constant voltage or constant current mode. In our experiment we use the constant voltage mode, as the plasma potential has to be constant for the purpose of beam extraction.

## B. Data acquisition system (DAS)

The DAS has 64 analog channels. It is designed to handle 128 MB of data in a single shot of 1000 s duration. The sampling rates for these channels can be varied from 1 ms to 10  $\mu$ s. The voltage and current signals from the various power supplies are acquired at a sampling rate of 1 kSa/s, which are acquired for the entire shot. We use a Langmuir probe in ion source to measure the density. The probe current, pressure signal, and single-filament heater current from the current transformer are acquired at the sampling rate of 100 kSa/s. For such measurements the data acquisition is event based, with the signals being acquired only for the region of interest. The currents of the discharge and heater power supplies are always monitored.

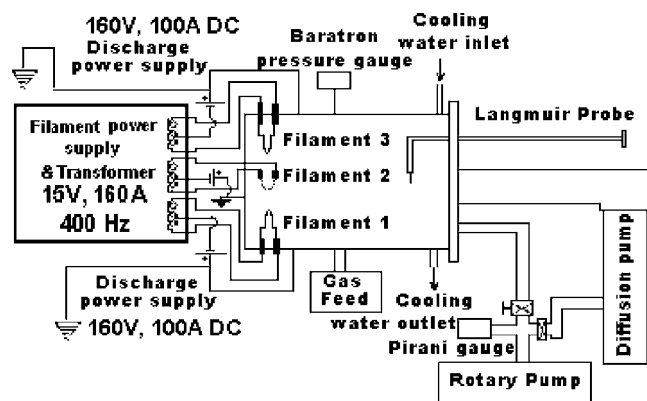


FIG. 2. Schematic diagram of experimental setup with electrical circuits.

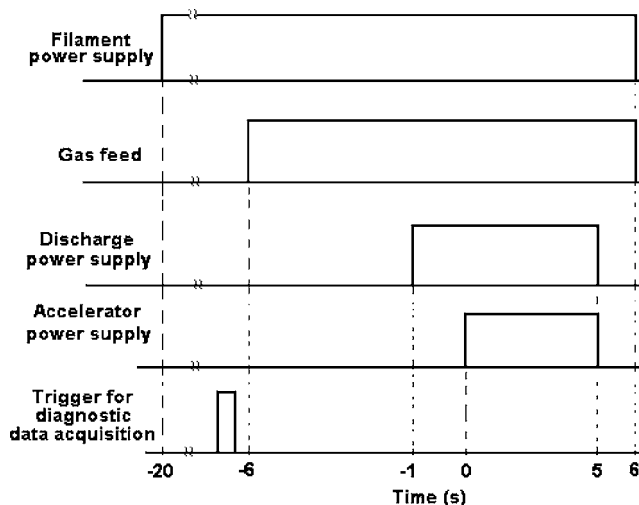


FIG. 3. Timing sequence for ion source operation.

## C. Requirement of control and timing system

The discharge current in the plasma box depends upon the gas pressure, the filament heater current, and the discharge voltage. These parameters are usually optimized through an iterative process to obtain good plasma, which is uniform over the extraction cross section within 5% and quiescent to fluctuations in plasma parameters (<5%). This is necessary to extract a uniform beam with a low divergence. The need for control arises from the fact that during the discharge, additional current passes through the filament. This causes additional heating which leads to changes in the plasma characteristics. The plasma characteristics can also change over a period of time because filaments become thinner as a result of evaporation. Usually the time scale of these changes is  $\sim 10^5$  s. Such variations can be adjusted by changing the set parameters. For tokamaks having operational time scales of tens of seconds, the need arises once in 2 to 3 months. With the introduction of 1000 s long machines, such changes may have to be made more frequently. In addition, the operation parameters may have to change online in response to plasma-wall interactions in the plasma box and in the tokamak.

The discharge current can be controlled by gas pressure, discharge voltage, and filament heater current. Changes in gas pressure can be implemented on the time scale  $> 100$  ms; therefore, it is not very useful. Voltage control leads to change in plasma potential. It will lead to variation in the beam extraction characteristics and is therefore not desirable. The control on filament heater current is the parameter most amenable to control.

In our ion source, the discharge current is controlled by the filament heater power supply. The AFC (arc discharge filament control system) enables one to keep the discharge current constant within 1% by reducing the heater current when filaments are heated by the discharge current as well. Feedback signals from the discharge current of all the filaments are acquired by the VME. Depending on the feedback, the system takes the appropriate action of adjusting the filament heater current to maintain constant discharge current. Control loop time in our experimental setup is a tunable

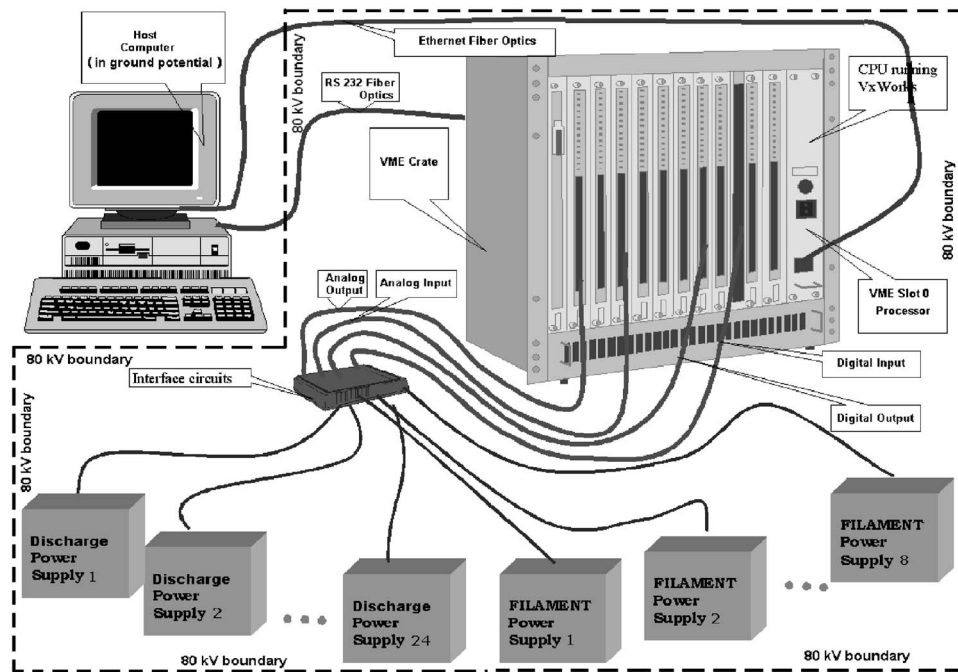


FIG. 4. VME system.

parameter. The VME-based control system not only controls the discharge current but also generates the timing for the overall operation of the NBI system. Triggers for the diagnostic data acquisition system, accelerator power supply system, as well as the gas feed control system, are also generated from the VME system at different times.

The present control system is tested for a beam pulse of 5 s, which later can be used for 1000 s operation. The limitation is that the prototype plasma box is not sufficiently

cooled to take 1000 s discharge pulses. The timing sequence for operating the ion source for 5 s is shown in Fig. 3. The filament power supply switches on with an initial set value of the current at  $t = -20$  s. This is followed by the start of the gas feed system at  $t = -6$  s. Discharge starts at  $t = -1$  s. At this time the control gets activated and lasts till the end of the pulse. The control system monitors and maintains the total discharge current by changing the filament voltage. At  $t = 0$  the accelerator voltage is applied. Before this event the discharge supply is open circuited for a short time (5 ms). At  $t = 5$  s the accelerator and discharge power supplies are switched off. This is followed by switching off of the gas feed system. Filament supply lasts for another 1 s before it is switched off.

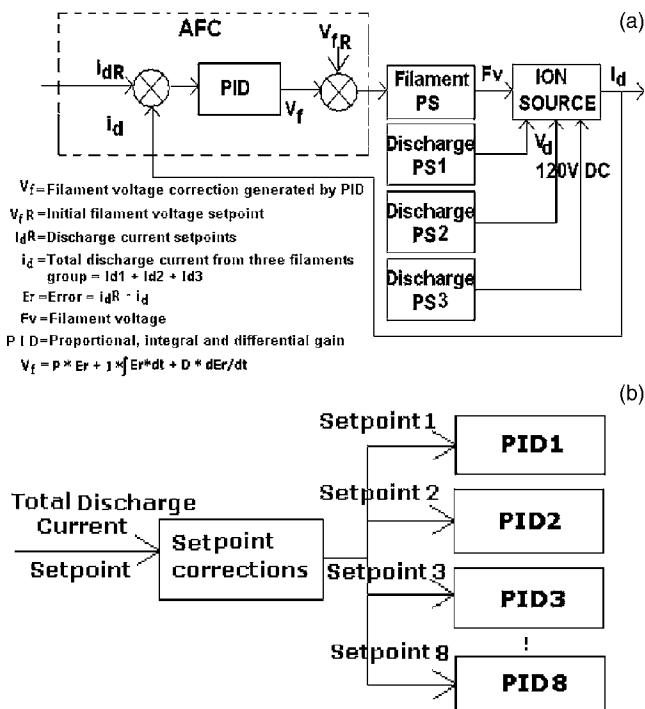


FIG. 5. (a) Single PID loop. (b) Overall PID controller with setpoint correction.

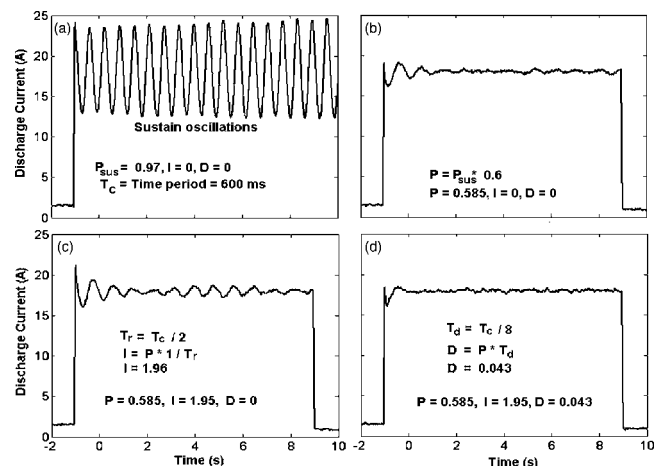


FIG. 6. PID tuning.

TABLE I. Software tasks and priorities.

Task number	Task name	Description	Priority number
1	DOTask	Sets the digital outputs to control the operation of the discharge and filament heater power supplies. Generates signals like START, WARMON, EMERGENCYSTOP	80
2	DOServerTask	Reads the command from the host computer and gives command to DOTask	80
3	DITask	Reads the digital input information from the power supplies and gives it to DIServerTask to send it to host computer	80
4	DIServerTask	Send digital input status to host computer	80
5	DAQTask	Perform the data acquisition and gives data to the control task to take control action	40
6	DataServer	Send data from VME CPU main memory to host computer for the postshot analysis.	80
7	TimingTask	Generate the timing information for the discharge, filament, high-voltage power supplies as well as trigger for gas feed system and diagnostics data acquisition system.	40
8	ConfigurationTask	Sets the initial reference voltage and current of the various power supplies	80
9	ConfigurationServer	Reads the configuration data from the host computer and gives it to ConfigurationTask.	80
10	ControlTask	Run 8 <i>PID</i> loops for AFC with setpoint correction loop.	40

### III. CONTROL SYSTEM

#### A. Hardware and software system configuration

The VME-based ion source AFC system uses a CPU 300 MHz Power PC 750, with other digital, analog, and timing modules. Digital I/O modules are used to monitor and operate the various power supplies under the control of the VME CPU module. The host computer is interfaced with the VME system using a fiber-optic Ethernet link. Analog-to-digital converter (ADC) modules have been used for the 64 channels. These modules have 32 channels each and a 12 bit ADC with overall sampling rate of 200 kSa/s. Each module has a 128 KB FIFO available to acquire the data continuously. One ADC module is triggered by the software and trigger output pulses are generated to synchronize other ADC modules. The acquired data are written to the FIFO memory. A block diagram of the VME system is shown in Fig. 4. The AFC system is floated at 80 KV and connected to the host at ground potential by optical fiber.

VxWorks<sup>TM</sup> operating system runs in the VME CPU module. The VME CPU loads the application software with VxWorks during the boot process from the host computer, through an Ethernet connection using the FTP protocol. The VME CPU module runs the application program to establish communication with other VME modules. The details of the software are described in the next section.

#### B. Control algorithm

The trigger from the operator panel starts the data acquisition using the two VME ADC modules. At every 1 ms interval a total of 160 data points (five samples per channel) per module are acquired at an overall sampling rate of 160 kSa/s. An average of five samples on each channel is

taken before it passes on to the control task to perform the processing of data. This reduces the effective sampling rate to 1 kSa/s per channel.

The control task reads the data from the acquisition task and analog output is generated by the VME module after processing of the data. As mentioned above, the power to the three filaments is fed from a single-filament power supply. Thus, a single reference voltage of the filament power supply adjusts the discharge current from the three filaments. Consequently, only eight control loops are needed to control the discharge current from 24 filaments. The schematic of the control algorithm used for the AFC is shown in Fig. 5(a).

Each *PID* control loop adjusts the filament voltage in order to change the filament current. We have eight such *PID* loops for 24 filaments. Figure 5(b) shows these loops with a

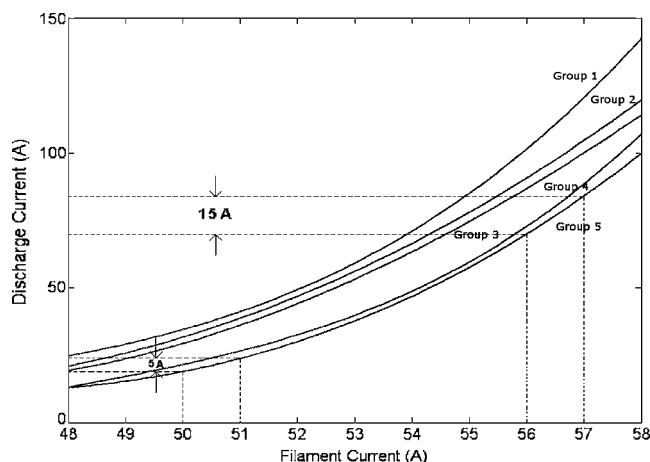


FIG. 7. Discharge current vs filament current obtained from different filament groups. A small change in filament current leads to a larger change in discharge current at higher filament current.

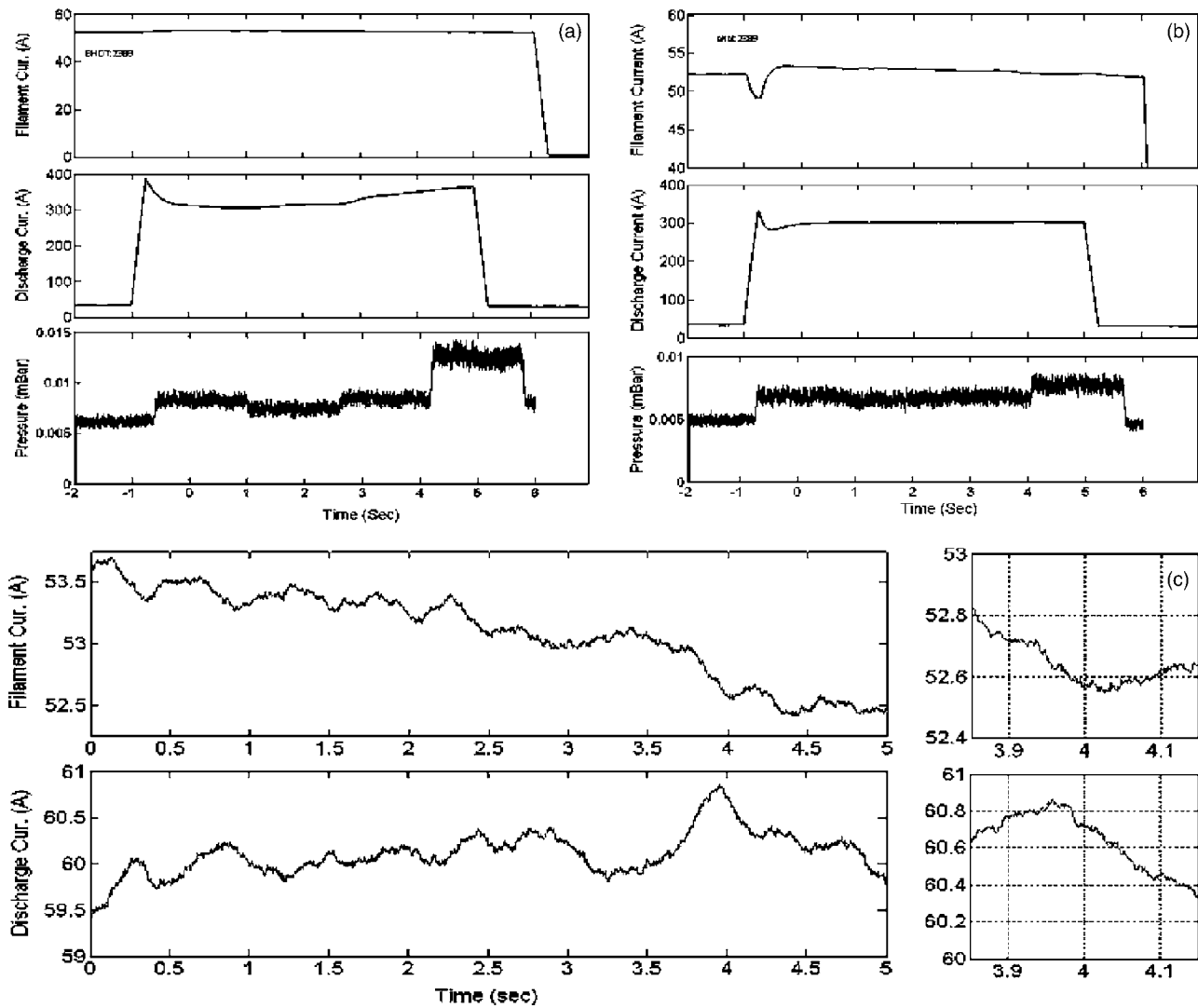


FIG. 8. (a) Without AFC, discharge current increases with the increase of pressure. (b) With AFC, discharge current remains constant in spite of pressure change. (c) Relation between discharge current and filament current with time reference.

setpoint correction. The setpoint of each *PID* loop is equal to one-eighth of the total discharge current. During the discharge, the setpoints of all the individual *PIDs* are corrected in case of failure of one or more filaments as described in Sec. IV.

### C. *PID* tuning

For *PID* tuning, open-loop as well as closed-loop methods are used. In our case the closed-loop method (Ziegler-Nichols method<sup>9</sup>) is preferred over the open-loop method. In the open-loop tuning method the gains are obtained based on the amplitude and the time delay of the process response for the step input. In our case, discharge current  $I_d$  is to be seen for the step change in filament current  $I_f$ . On the other hand, the closed-loop system is frequency dependent. The *PID* gains are derived for a given value of the *P* gain for which sustained oscillations have been obtained. The  $I_d$  is related to the filament temperature  $T_f$  by the Richardson-Dushman equation.

$$I_d \approx I_{em} = AT_f^2 \exp\left(-\frac{\phi}{kT_f}\right) a_f \quad (1)$$

$$T_f^2 = \left(\frac{R}{\sigma \epsilon_0 a_f}\right)^{1/2} I_f \quad (2)$$

where  $I_{em}$ =electron emission current,  $A=1.2 \times 10^6 \text{ Am}^{-2} \text{ K}^{-2}$  (Richardson constant),  $\phi$  is the work function of the filament material,  $k$  is the Boltzmann constant,  $\sigma$  is the Stefan constant,  $\epsilon_0$  is the emissivity of the filament,  $a_f$  is the filament surface area,  $I_f$  is the heater current, and  $R$  is the resistance of the filament.

As seen from the above equation, the relationship between  $I_d$  and  $I_f$  is inherently nonlinear. As shown in the experimental results of Sec. IV, the increment in  $I_d$  is different for different values of  $I_f$ . Hence, for the open-loop case, the *PID* gains will have to be optimized for different ranges of the heater current, which is a major drawback.

Our AFC is a closed-loop control system, with closed-loop time of 20 ms. For a response time of  $\sim 30$  ms for our filament heater power supplies, reducing the *PID* loop time  $< 20$  ms will not be a useful exercise. The ultimate *P* gain for which we get sustained oscillations (with ultimate frequency=1.7 Hz) on discharge current is 0.97. During this exercise  $I=0$  and  $D=0$  and the discharge current oscillates

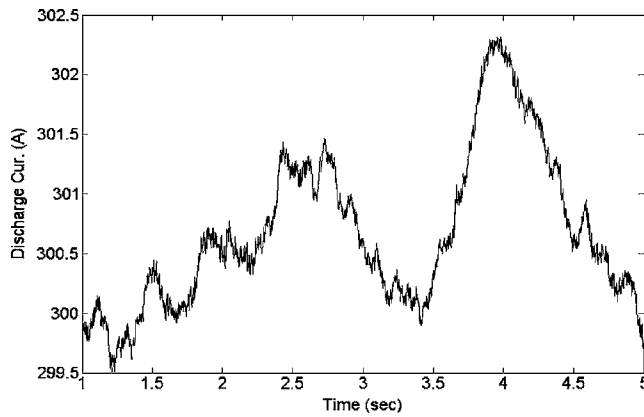


FIG. 9. Total discharge current and its fluctuation with time.

around the setpoint [Fig. 6(a)]. It may be noted that the setpoint in the discharge current is set to 18 A and the shot duration is 10 s. From these values of the ultimate gain and ultimate frequency we have calculated the  $P$ , the  $I$ , and the  $D$  gain by using the following equations:

$$P = P_{\text{sus}} \times 0.6, \quad (3)$$

$$I = P \times 2/T_c, \quad (4)$$

$$D = P \times T_c/8, \quad (5)$$

where  $P_{\text{sus}}$ =ultimate  $P$  gain and  $T_c$ =ultimate time period. Using  $P_{\text{sus}}=0.97$  and  $T_c=600$  ms, we obtained gains ( $P=0.585$ ,  $I=1.95$ , and  $D=0.043$ ); a control on the discharge current without any oscillation has been observed. Figures 6(b)–6(d) show the response of the system for  $P$ ,  $PI$ , and  $PID$  gain settings. In our ion source, the gain of  $D$  has been further increased by 1% to get a smoother discharge. These values have been used for all our experimental measurements on the ion source. These values are seen to hold well for the long-duration shot (>100 s) and shots involving different discharge current setpoints.

#### D. Control software

VxWorks is run under the VME CPU module. VxWorks is a real-time operating system. It has interrupt latency time <100  $\mu$ s with Power PC VME CPU. Data acquisition and control software has been embedded with the VxWorks operating system. This software starts running after the VME CPU boot process is over. The complete software has been subdivided into many tasks. In VxWorks the higher the priority number, the lower is the functional priority. Various tasks

and their functions are described in Table I. These tasks communicate with each other by the message queue and pipe. They are synchronized by semaphores. The priorities are assigned depending upon the functionality of the task. The data acquisition and the control task are assigned the highest priority. The data acquisition task initiates the data acquisition and transfers the acquired data in 1 ms from the FIFO to the VME CPU main memory after receiving the interrupt from the timer module. The data are then available to the control task to take the desired corrective action. Communication with the host computer is done by the server tasks, which have the lowest priorities.

The host computer graphical user interface (GUI) is developed using LabWindows/CVITM, which uses C programming language with a graphical library. This is used to set all operating parameters (voltage and current) of the discharge and the filament power supplies and to monitor the reference voltages and the current.

#### IV. PERFORMANCE OF THE AFC SYSTEM

Figure 7 shows the variations of the discharge current with filament current for a case where 15 filaments and five filament heater power supplies have been used. The filaments have a diameter of 1 mm. It is seen that for a filament heater current ( $I_f$ ) up to 50 A, the discharge current ( $I_d$ ) increases by 5 A for a 1 A increase in the filament heater current. For  $I_f > 50$  A, an increment in  $I_f$  by 1 A shows a corresponding increment of  $\sim 15$  A in  $I_d$ . This implies that a sensitive control with high resolution is needed for the setting of the filament heater current.<sup>10</sup>

The effect of pressure variation on the discharge current is shown in Fig. 8(a). On application of the discharge voltage, the discharge current shoots up momentarily, followed by a decrease to the stable value. As discharge progresses, the chamber walls are heated up and the adsorbed gas on the walls is released. This results in an increase of the chamber pressure, which is monitored by a Baratron gauge. As a result the plasma density also increases. Since the device is operated in a constant voltage mode, the discharge current cannot be maintained constant because of degassing of hydrogen from the walls.

When we apply AFC, the  $PID$  controller running in VME adjusts the filament currents. Both the power supplies are running under the CV mode. But, filament power supplies output voltage which is adjusted to control the discharge current. Figure 8(b) shows the discharge and the filament currents during a single run when AFC is applied. The

TABLE II. Adjustment of setpoints in the filaments failure scenarios.

Group 1	Group 2	Group 3	Group 4	Group 5	Total discharge	Bad filaments	Remark
60 A	300 A	0	All filaments are working				
64.2 A	64.2 A	42.8 A	64.2 A	64.2 A	300 A	1	Group 3 has one bad filament
46.1 A	69.2 A	46.1 A	69.2 A	69.2 A	300 A	2	Group 3 and Group 1 have bad filament

*PID* decides the new value of the filament voltage. We notice that the filament current decreases by 5 A to overcome the initial overshoots in the discharge current. Finally, the discharge current converges to the setpoint, which is 300 A for the results shown in Fig. 8(b). Each group of three filaments supplies discharge current of 60 A. The chamber pressure is seen to increase after 2 to 3 s of the discharge. In this event the filament current decreases by  $\sim 1.5$  A to maintain the discharge current at setpoint. Figure 8(c) shows the variation of filament current and discharge current for a single group of three filaments. Excellent correlation is observed between the  $I_f$  and the  $I_d$ . The total control is exercised by  $I_f$  and any variation in  $I_d$  due to variation in other parameters, like pressure due to ion flow or wall degassing and discharge current, can be countermanded by effecting control on  $I_f$ . It may be noted that in the event of the discharge current crossing the setpoint in either direction, the filament current adjusts itself to maintain the discharge current at setpoint. The variation of  $I_f$  is within a narrow range ( $\sim 0.2$ – $0.4$  A). For a 5 s shot, the filament current reduces by 1.5 A. The peaks and valleys of the filament current and discharge current are exactly anti-correlated. The difference between the discharge current peak and filament current valley is  $\sim 60$  ms. Figure 9 shows the total discharge current from 15 filaments (5 groups). It varies between 299 and 302 A around a setpoint of 300 A, showing thereby a variation of  $\leq 1\%$ .

When a single filament of the group does not contribute to the discharge current due to filament breakdown or the power supply problem, the setpoint of this group is reduced and the reduction in the discharge current is compensated by a corresponding increase from other groups. Table II shows the different setpoints of the group when a single filament of one group or multiple groups malfunctions. A maximum of up to five bad filaments from different groups is allowed. If more than one filament in a single group is bad, the control shuts off the system and the filaments have to be replaced.

An overshoot in the discharge current is observed on application of the discharge voltage at  $t = -1$  s. Sometimes this overshoot is as high as 50% of the total discharge current. The overshoot can be controlled by effectively controlling the rise time of the discharge current. This can be achieved by fine-tuning the gains of the *P*, *I*, and *D* and also by starting with low quiescent value of the filament current. As seen in Fig. 10, the rise time of the discharge current is  $\sim 1.5$  s for a setpoint of 250 A.

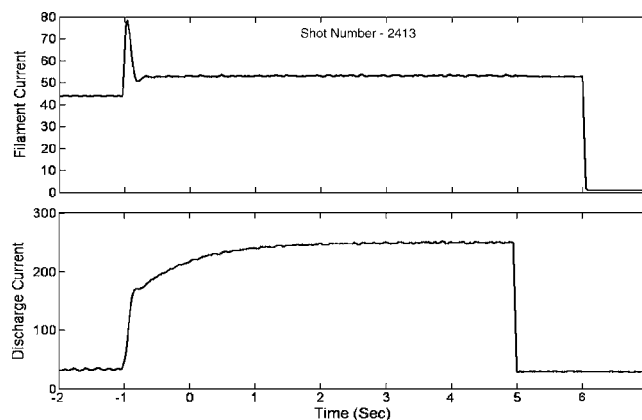


FIG. 10. Longer rise time in discharge current.

## V. DISCUSSION

AFC, which is the most important requirement for the steady-state operation of the ion source, has been successfully implemented using VME with VxWorks operating system. *PID* is running under the VxWorks. *P*, *I*, and *D* gains have been optimized by fine-tuning of the *PID*. As the *PID* is software based, no modification in the hardware components is required and the parameters can be easily changed by the operator. In our case, VME has not just been used for the AFC to control the discharge current variation to  $< 1\%$  during the discharge but has also been utilized for the purpose of status monitoring of the power supplies, the data acquisition, and the timing system for the whole NBI. The *PID* loop also protects the filaments as it never allows the heater currents to exceed the set limits.

## ACKNOWLEDGMENT

The authors would like to thank P. Ganshani and P. Bakeri from Nirma Institute of Technology, Ahmedabad for their help for sourcing *PID* tuning method.

- <sup>1</sup>S. G. Lee *et al.*, Rev. Sci. Instrum. **70**, 1397 (1999).
- <sup>2</sup>SST1 Team, 16th IEEE/NPSS Symposium on Fusion Engineering Urbana, IL, 30 September–5 October 1995, Vol. 1, p. 481.
- <sup>3</sup>S. Idle and JT-60 Team, Phys. Plasmas **7**, 1927 (2000).
- <sup>4</sup>A. Becoulet *et al.*, AIP Conference Proceedings 485, 302 (1999).
- <sup>5</sup>J. A. Boedo *et al.*, Phys. Plasmas **7**, 1075 (2000).
- <sup>6</sup>A. Loarte *et al.*, Phys. Rev. Lett. **83**, 3657 (1999).
- <sup>7</sup>W. Tenten *et al.*, Proceedings of 17th Symposium on Fusion Technology, Vol. 2, p. 1086 (1993).
- <sup>8</sup>J. R. Luo, Nucl. Fusion **43**, 862 (2003).
- <sup>9</sup>L. M. Zoss, *Applied Instrumentation in the Process Industries* (Gulf Publishing Co., 2002).
- <sup>10</sup>D.-H. Change, Plasma Sources Sci. Technol. **14**, 336 (2005).